

A computational tool for identifying minimotifs in protein–protein interactions and improving the accuracy of minimotif predictions

Sanguthevar Rajasekaran,^{1*} Jerlin Camilus Merlin,¹ Vamsi Kundeti,¹ Tian Mi,¹ Aaron Oommen,¹ Jay Vyas,² Izua Alaniz,³ Keith Chung,³ Farah Chowdhury,³ Sandeep Deverasatty,³ Tenisha M. Irvey,³ David Lacambacal,³ Darlene Lara,³ Subhasree Panchangam,³ Viraj Rathnayake,³ Paula Watts,³ and Martin R. Schiller³

¹ Department of Computer Science and Engineering, University of Connecticut, Storrs, Connecticut 06269-2155

² Department of Molecular, Microbial, and Structural Biology, University of Connecticut Health Center, Farmington, Connecticut 06030-3305

³ School of Life Sciences, University of Nevada Las Vegas, Las Vegas, Nevada 89154-4004

ABSTRACT

Protein–protein interactions are important to understanding cell functions; however, our theoretical understanding is limited. There is a general discontinuity between the well-accepted physical and chemical forces that drive protein–protein interactions and the large collections of identified protein–protein interactions in various databases. Minimotifs are short functional peptide sequences that provide a basis to bridge this gap in knowledge. However, there is no systematic way to study minimotifs in the context of protein–protein interactions or vice versa. Here we have engineered a set of algorithms that can be used to identify minimotifs in known protein–protein interactions and implemented this for use by scientists in *Minimotif Miner*. By globally testing these algorithms on verified data and on 100 individual proteins as test cases, we demonstrate the utility of these new computation tools. This tool also can be used to reduce false-positive predictions in the discovery of novel minimotifs. The statistical significance of these algorithms is demonstrated by an ROC analysis ($P = 0.001$).

Proteins 2011; 79:153–164.
© 2010 Wiley-Liss, Inc.

Key words: *Minimotif Miner*; *Homologene*; *BLAST*; *Grb2*; *SLiM*; *short linear motifs*.

INTRODUCTION

Protein–protein interactions (PPIs) are central to understanding how cell functions are integrated. At this point, scientists have deciphered a well-developed theory that explains the physical and chemical forces that underlie the noncovalent chemistry of PPIs. Electrostatic, dipole–dipole, van der Waals forces are well quantified into accepted force fields such as AMBER that are used for protein structure determination by NMR, modeling of macromolecules, refinement of X-ray structures, macromolecular dynamics, and drug design.^{1–3} A more recent knowledge base of PPIs has emerged from the growing number of PPI databases built upon data largely from high-throughput techniques such as yeast two-hybrid screens and tandem affinity purification/mass-spectrometry analysis, as well as manual curation of the scientific literature. Collectively BIND, DIP, BioGrid, IntAct, MIPS, MINT, HPRD, the YPD and others contain several hundred thousand PPIs.^{4–8} Despite these efforts, we are yet to develop a comprehensive enumeration of PPIs.

One of the major efforts addressing the development of a theory that reliably predicts new PPIs is that of minimotifs (also called short linear motifs or SLiMs), which bind to protein domains and provide a key connection of the physical and chemical forces with the large PPI data sets. Minimotifs are contiguous peptide elements in proteins, generally less than 15 residues in length that have a defined function. One class of functions includes binding minimotifs such as those that engage SH2, SH3, PDZ, and a number of other modular protein domains.⁹ These minimotifs are

Additional Supporting Information may be found in the online version of this article.

Sanguthevar Rajasekaran and Jerlin Camilus Merlin contributed equally to this work
Grant sponsor: National Institutes of Health; Grant number: GM079689; Grant sponsor: NSF; Grant number: 0829916; Grant sponsor: Universities of Nevada Las Vegas and Connecticut.

*Correspondence to: Sanguthevar Rajasekaran, Department of Computer Science and Engineering, University of Connecticut, Storrs, CT 06269-2155. E-mail: rajasek@engr.uconn.edu or Martin R. Schiller, School of Life Sciences, University of Nevada Las Vegas, 4505 Maryland Parkway, Las Vegas, NV 89154-4004. E-mail: martin.schiller@unlv.edu.

Received 23 April 2010; Revised 22 July 2010; Accepted 13 August 2010

Published online 9 September 2010 in Wiley Online Library (wileyonlinelibrary.com).

DOI: 10.1002/prot.22868

of known molecular function and are distinct from *de novo* prediction of motifs by several approaches including MEME, Gibbs Sampler, PRATT, TEIRESIAS, D-MOTIF, and other algorithms.^{10–14}

While some PPIs involve extensive surface contact, PPIs driven by minimotifs are generally simpler, with a reduced surface of contact. Analysis of minimotif-driven PPIs simplifies the problem of theoretically predicting new PPIs by limiting the residues that need to be considered. In general, minimotifs are identified by studying sequences of a collection of instances that are known to interact with a protein or by analysis of the permutational space of each position in a peptide sequence that can bind to a domain by phage display, screening random peptide libraries, SPOT peptide arrays, or site-directed mutagenesis. Most often interpretation of this data reduces the series of instances down to a consensus minimotif that accounts for degeneracy at each position. Alternatively, degeneracy and variation can be quantitatively represented in a position specific-scoring matrix (PSSM), which has the advantage that it captures the probability of the collection of instances for each position.

Consensus sequences and PSSMs have some predictive value but have limitations. While high-throughput experimentation has helped us to begin to understand some of the specificity determinants of many minimotifs, sequence alone is not an accurate predictor of novel minimotif instances and does not, by itself, account for the higher degree of specificity observed in minimotif-driven PPIs.

There has been much effort to increase the specificity of and reduce false-positive minimotif predictions.^{15–19} In the Minimotif Miner (MnM) application for predicting minimotifs, three approaches can be used: frequency analysis relies on the simple premise that minimotifs with more complex definitions are less likely to have false-positives.^{15,16} Since minimotifs must be on the surface of a protein, a surface prediction algorithm can be used to minimize the prediction of buried minimotifs. Likewise, those minimotifs that are conserved in different species provide another measure to reduce false positives. Another major minimotif database, eukaryotic linear motif (ELM) server utilizes different filters that are complementary to MnM.^{17,18} A cell compartment filter identifies minimotifs in appropriate cellular compartments, while a globular domain filter can be used to restrict predictions to intrinsically disordered regions. ELM uses taxonomy in a different way than MnM to identify minimotifs in organisms with a conserved minimotif partner. ELM also has a surface filter and a secondary structure prediction filter.

In MnM a query protein (minimotif source protein) is entered and, in part, the sequence is analyzed for minimotifs that encode putative interactions with target proteins. Each query generally produces many target predictions; however, like other minimotif prediction programs, there is a relatively high number of false-positive predictions. To address this limitation, we have now adapted a concept previously used to identify novel minimotifs.¹⁹ Neduva

and Russel¹⁹ examined sets of protein–protein interactions to identify proteins that interacted with a common target protein and shared a unique minimotif signature.

Here, our goal was to engineer a new tool that would have two principle uses: (1) it would improve prediction of new minimotifs in MnM, by reducing the false-positives predictions. A filter would restrict the target predictions to those proteins where the minimotif source protein and the target protein are already known to interact. We implemented several strategies to modulate filter stringency. (2) It can be used to facilitate the study of PPI theory by identifying minimotifs between two proteins that are already known to interact, but the interface is not yet known. For example, in an example analysis of discs, large homolog associated protein (DLGAP-1, NP_075235) Minimotif Miner predicts 123 potential binding motifs; however, only two are previously known to have a known protein–protein interaction. Thus, using PPIs reduced the number of minimotif predictions. In the second application mentioned earlier, an example analysis of DLGAP-1 shows that it contains PxxPxK and YxxP minimotifs. These minimotifs are known to bind to the SH3 and SH2 domains of Crk, respectively.²⁰ A protein–protein interaction of DLGAP1 with Crk was previously identified by an array screen of SH3 binding motifs that included Crk peptides.²¹ Thus, two mechanisms for this PPI are now suggested.

METHODS

Protein–protein interaction filters

To refine minimotif predictions using known PPIs, we first needed sources of protein–protein interaction data. The minimal PPI data we need is two interacting proteins with accession numbers. We accepted the limitation that some protein–protein interaction databases may contain data with a low intrinsic false-positive rate, containing a few incorrect or artifactual interactions. We selected six databases primarily based on the public availability, amount of data, and reliability of the data. The Database of Interacting Proteins (DiP), Entrez Gene, Human Protein Resource Database (HPRD) release 8, Molecular Interaction database (MINT) release 2.5, VirusMINT and IntAct contain protein–proteins interactions annotated from the literature or derived from experimentation.^{5,22,23} Statistics for these databases are provided in Table I.

Collectively, these databases have >785,000 total interactions. The total number of nonredundant interactions is likely more similar to the 322,579 unique PPIs consolidated in the Agile Protein Interaction DataAnalyzer.⁸

Annotation of minimotifs

All minimotifs in the Minimotif Miner database were curated from the literature and have supporting

Table 1
Sources of Protein–Protein Interaction Data

Database	No. of interactions	No. of proteins	No. of species	Data source	Reference	Date downloaded
DiP	57,683	20,728	274	Literature curation	37	Aug., 2009
Entrez Gene	387,159	19,205	Unknown	Linkout databases	38	Sep., 2009
HPRD	38,806	27,081	1	Yeast 2-hybrid, <i>in vitro</i> or <i>in vivo</i> experiments, proteinpedia	39	Aug., 2009
MINT	83,321	29,774	Unknown	Literature curation	40	Jun., 2009
Virus MINT	1,854	468	99	Literature curation	23	Nov., 2009
IntAct	216,394	63,654	Unknown	Experiments	22	Jun., 2010
Total ^a	785,217					

^aTotal does not consider that different databases may use different accession numbers for the same protein.

experimental evidence.^{15,16} The data was refactored into a new data model.²⁴ The basic elements of this model have a “motif source,” which contains the Minimotif, a “target,” which engages the Minimotif, and an “activity” which describes the function outcome of the minimotif source engaging its target. To use this information for the computational PPI filters, we examined the references for all 5313 minimotif definitions and assigned accession numbers to the majority of Minimotif sources and targets. In a few cases the accession number could not be assigned for one of two reasons: (1) an unambiguous assignment could not be made based on the information in the paper or in referenced material, or (2) if the minimotif source was identified in a phage display, or peptide-based screen then there is no assignment of an accession number.

Protein–protein interaction filtering algorithms based on homology and similarity

We designed several protein–protein interaction filtering algorithms that could be compared for their utility in refining minimotif definitions. The basic algorithm is as follows: For the purpose of describing these algorithms, let p be the putative minimotif, let S be its source protein, and let T be the target protein which interacts with the source protein that contains p as previously described in our model of minimotifs.²⁴ Each PPI pair will be assigned to (A, B) and (B, A) where A and B are proteins, thus there are two assignments to (S, T) for each PPI. Then each database is searched for an exact (S, T) match. This filter is designated the “PPI-filter.”

The source of minimotifs for this analysis will be the minimotif miner (MnM) database, which has over 3000 minimotifs for protein–protein interactions and is modeled with pairs of minimotif source and target proteins (S, T) .^{15,16} To use MnM for this filter, we annotated both source and target accession numbers for all of the ~3000 PPI minimotifs that could be unambiguously assigned.

Several studies suggest that the minimotifs that drive PPIs are often conserved between species.^{25–27} There-

fore, we designed an extension of the above protein–protein interaction filter, designated the “HomoloGene-PPI” filter that uses the HomoloGene database to extend PPI predictions into other species. HomoloGene is a database, which clusters paralogues and orthologues into gene families.²⁸ For a given (A, B) pair in a PPI database, we can assign (A_i, B_i) and (B_i, A_i) to (S_i, T_i) , where i indicates a species. We examine HomoloGene clusters for S_i and then match the species to T_i , which evaluates both proteins of a (A, B) pair. Using this approach, we can now expand the number of PPI interactions based on the assumption that the interactions are conserved in orthologues and paralogues across species and taxa.

While the HomoloGene-PPI filter assesses conservation in orthologues and paralogues, minimotifs may also be conserved in a broader range of homologues. For example, a PxxP minimotif is likely to bind to many of the 100’s of SH3 domains present in different proteins, even if the proteins are homologues in the same species. To develop this “Similarity-PPI” filter, we used all the protein–protein interaction databases. Each protein in these databases was used to form a cluster using BLAST.²⁹ Each cluster will have proteins with sequence similarity. By varying the threshold cutoff value in the BLAST analysis, we generated clusters with different stringency. We refer to these versions of PPI databases as Extended-PPI. A pair in the extended-PPI is of the form (A, B') or (A', B) where A and B are proteins and A' and B' are protein clusters. In the Similarity-PPI filter, for any given source target pair (S, T) , all the entries in the database are examined to identify interacting protein–protein pairs (S', T') where S' is similar to S and T' is similar to T . A pseudocode for the detailed algorithm is given in the Appendix. To reduce false positive predictions of PPIs by this approach, we optionally enforced the additional constraint that S' should contain p , the putative motif.

ROC curves

Relative operating characteristic (ROC, also named receiver operating characteristic) curves are commonly used to evaluate the sensitivity and specificity of

algorithm performance and were used to evaluate the PPI filters. We used the R project software suite to compare ROC curves of the PPI filter with the frequency score filter used on the MnM website.³⁰ In the R package, the area under the curve (AUC) is calculated following Mason and Graham's methods.³¹ The ROC area can be interpreted as re-parameterized forms of the Mann–Whitney U -statistic.³² The statistical significance (P -value) of the ROC area is calculated from the Mann–Whitney U -distribution. In this article, AUC and P -values are calculated based on empirical curves. We have compared the empirical curves to a ROC curve fit with a binormal function, which assumes that the positive data follow a normal distribution. The robustness of binormal model shows high similarity with experimental curves, even when the data follow some other distribution.³³

RESULTS

Evaluation of protein–protein interaction filters

We wanted to create a set of filters that reduce the number of false-positive minimotifs predicted by Minimotif Miner. Given a query protein, we plan to use PPI filters to restrict these predictions to those that are previously known to have a PPI. We also generated and tested less stringent versions of these filters (PPI-HomoloGene, and PPI-Similarity). The PPI, PPI-HomoloGene, and PPI-Similarity filtering algorithms were evaluated using the Minimotif Miner 2 (MnM2) database. MnM2 has 2941 PPI minimotifs where accession numbers for both the minimotif source protein (that contains the minimotif) and the target protein (that binds to this minimotif) are known. We used two metrics to evaluate the success of these filters.

To assess sensitivity of these filters, the percentage of protein pairs that were identified in both a PPI database and MnM database was computed. This percentage metric can be thought of as the *sensitivity* of the algorithm filter with higher percentage recovery representing higher sensitivity.

We also wanted to test the selectivity of each filter for true minimotifs. We randomly selected 100 proteins to be processed using MnM. Let A be one such query protein. A list L of putative minimotifs identified by MnM was collected. Let r be an entry in L . Let the target protein for the r motif in A be T . We sent (A, T) to the PPI filter and checked if this pair will pass the filter (that is, we sent a minimotif-containing protein and an interaction partner predicted by MnM into the PPI algorithm). We did this for every element in L generated by MnM for the 100 randomly picked proteins. As a result, we computed the percentage of minimotifs (r 's) known to mediate binding with targets (T 's) contained in the 100 proteins (A 's). This is the percentage of interactions (A, T) , which passed the filter. We refer to this percentage as

Table II
Evaluation of the PPI Filter

	Sensitivity ^a (%)	Selectivity ^b (%)	Discrimination ratio ^c
DIP	1.6	0.0	x
Entrez Gene	40.7	3.3	12.5
HPRD	31.0	2.7	11.6
MINT	41.2	1.5	27.7
VirusMint	0.2	0.0	x
IntAct	7.4	0.7	11.4
At least one ^d	61.6	2.1	29.3

^a“Sensitivity” refers to the percentage of positive instances that are accepted by the filter.

^b“Selectivity” refers to the percentage of negative instances accepted by the filter.

^c“Discrimination ratio” is sensitivity/selectivity.

^d“At least one” refers to a minimotif that was identified in at least one of the PPI databases listed in this table.

the *selectivity* of the filter; lower numbers indicate more selectivity for valid minimotifs. We use the ratio of *sensitivity/selectivity* as a single metric called discrimination ratio (DR) that evaluates the success of the filter.

Since we did not know the redundancy and coverage of each PPI database, the PPI-filter was evaluated for each of the PPI databases (Table II). The results obtained for MINT, HPRD, and Entrez Gene database showed that many PPIs were also present in MnM; whereas few were identified in a set of randomly synthesized PPI interacting pairs; this is reflected as higher sensitivity. Collectively, 58% of minimotifs had a PPI in at least one of the six PPI databases examined. We compared the results of the filter using MINT, HPRD, and Entrez Gene databases with a set of randomly synthesized PPI interacting pairs. Overall, integration of all six PPI databases yielded the highest overall Discrimination Ratio of 31 (higher scores indicate better performance), revealing the effectiveness of this filter and suggesting that when applied to novel queries this filter would help to reduce false positive predictions.

We next evaluated the HomoloGene-PPI filter to determine if extending the sets of PPIs to include orthologues and paralogues reduces the stringency of the PPI filter. The HomoloGene-PPI filter did not produce any significant increase in sensitivity when the MnM data set was analyzed; however, there was a modest reduction of selectivity reducing the Discrimination ratio score when compared to the PPI filter (Table III). The reason that the HomoloGene-PPI did not yield major improvements is likely because there are few minimotifs in the MnM data set where a minimotif in an interaction is defined for more than one species. Although this algorithm did not improve results in analysis of the MnM data set, we can envision situations where this filter is valuable as shown applying this filter to a test case in the next section.

To further reduce stringency of the PPI filter, we created and tested the Similarity-PPI filter, which uses BLAST instead of HomoloGene clusters to identify proteins with sequence similarity. The BLAST threshold used to identify similar proteins was varied and the performance of this

Table III
Evaluation of the HomoloGene-PPI Filter

	Sensitivity ^a	Selectivity ^a	Discrimination ratio ^a
DIP	1.9	0	x
Entrez Gene	44.7	3.5	12.7
HPRD	33.3	2.7	12.2
MINT	41.2	2.4	17
VirusMint	1.5	0	x
IntAct	8.3	1.2	7
At least one ^b	63.7	5.1	12.5

^aMeasurements in column are as defined in Table I.

^b"At least one" refers to a minimotif that with a source and target that matched in at least one of the PPI databases listed in this table.

filter was assessed as for the other filters (Fig. 1). The discrimination ratio (sensitivity/selectivity) correlated positively with increasing BLAST scores, indicating that the more stringent the sequence similarity, the better the filter performance. The discrimination ratio was better than that of the HomoloGene-PPI filter when BLAST thresholds above 20 were used.

Better selectivity scores were obtained when using high BLAST thresholds with the Similarity-PPI filter. With BLAST thresholds of 10 and 20 we observed increases in sensitivity as well as less stringent selectivity. However, the gains in selectivity were not sufficient to improve the overall DR. This was expected when a wider breadth of homologues is selected with lower BLAST scores selectivity should become worse. The potential use of this filter is that it is capable of generating broader (albeit less stringent) predictions of minimotifs than either of the PPI and HomoloGene-PPI filters.

An ROC curve was used to assess the Similarity-PPI filter; the underlying variable parameter was the BLAST score. Note that for PPI-filter and HomoloGene-PPI filter there is

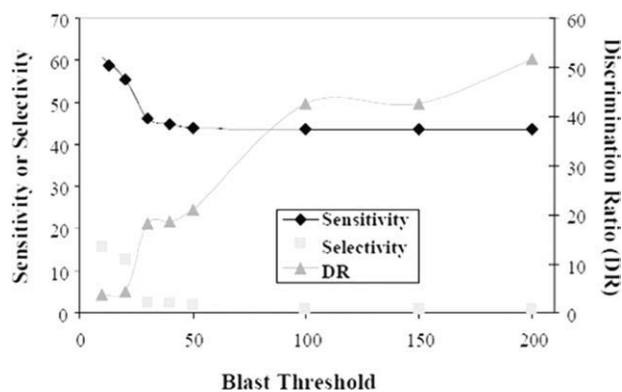


Figure 1

Evaluation of the BLAST threshold used to create extended-MINT in the Similarity-PPI filter. The Similarity-PPI filter was applied to various datasets and sensitivity, specificity, and the discrimination ratio were measured and plotted. Different datasets were created using BLAST to identify proteins with sequence similarity; the BLAST threshold was varied.

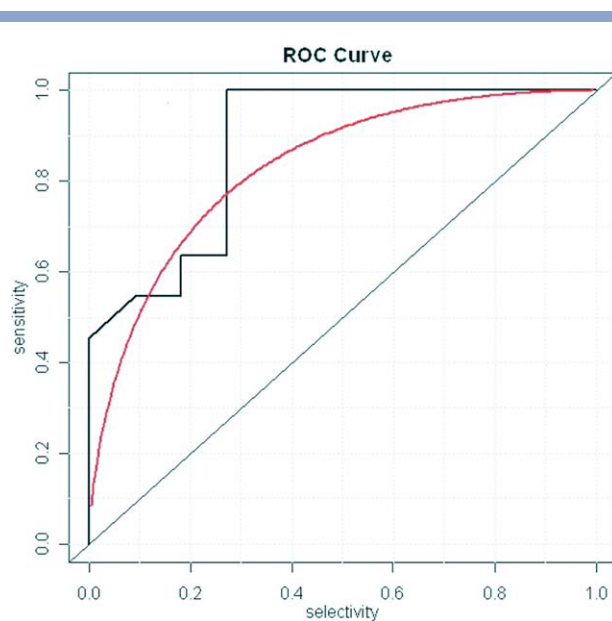


Figure 2

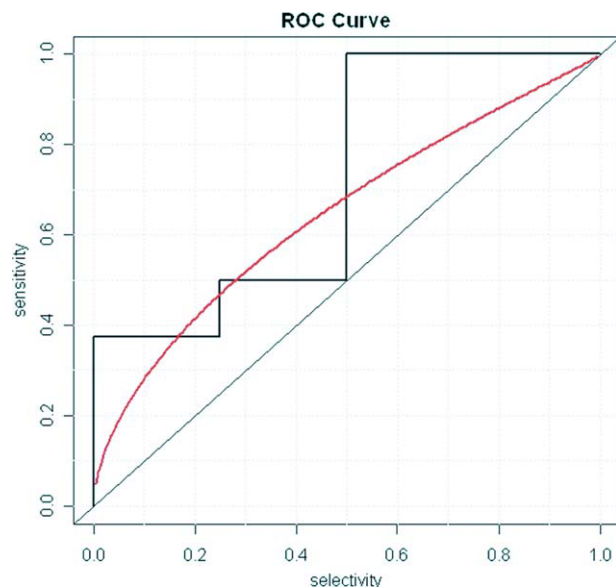
ROC curve for Similarity-PPI Filter. ROC curves for the Similarity-PPI curve were generated with the R project software package. The empirical curve (black) and binormal curve (red) are shown. The binormal curve is calculated based on the assumption that the data is from a normal distribution. The area under the empirical curve is 0.9 ($P = 0.001$).

no such parameter and hence ROC curves are not relevant. This ROC curve (Fig. 2) clearly demonstrates the statistical significance of our algorithm. The area under the curve is 0.9 and the P -value is 0.001. Note that the P -value corresponds to the probability that a random predictor (i.e., filter algorithm) will produce the same results as our algorithm. We also wanted to compare the performance of our algorithm in relation to the existing frequency filter of MnM. The frequency score filter scores minimotifs based on the amino acids in the minimotif sequence definition and the frequency of these amino acids in the proteome.¹⁵ The area under the ROC curve for the frequency filter is 0.7, and the P -value is 0.08 (Fig. 3). Comparison of ROC curves for the two filters shows that the PPI filter has a better performance than the previously reported frequency score filter.¹⁵ Table IV compares these two filters on many parameters of interest. In this table, n_{total} is the total number of tests, n_{events} is the total number of tests on true data, $n_{noevents}$ is the total number of tests on random (negative) data.

The other principle goal was to identify minimotifs that are present in one of two proteins known to interact. By using any of these filters on the MnM website users can enter a query protein and use MnM to find a minimotif that potentially drives the mechanism of the interaction.

Examination of Grb2 using PPIs

To further test the different PPI filters, we examined growth factor receptor binding protein 2 (Grb2) as an

**Figure 3**

ROC curve for Frequency Score Filter. The Frequency Score Filter previously implemented in MnM was analyzed and an ROC curve was plotted for the sensitivity and specificity of the filter by varying the frequency threshold. Curves are as in Figure 2. The area under the empirical curve is 0.7 ($P = 0.08$). [Color figure can be viewed in the online issue, which is available at wileyonlinelibrary.com.]

example minimotif source query. Grb2 is an adaptor protein involved in receptor tyrosine kinase signaling that has many known protein interaction partners, thus provides a good test case. We analyzed Grb2 proteins from human, mouse, rat, and fly and indicate the percentage of the minimotifs that pass the filter (Table V). With the PPI filter 36% of the predicted minimotifs for human and 13% of rat Grb2 had previously known interactions; fly and mouse Grb2 has not reported minimotifs with known PPIs in the MnM database. The PPI filter would provide benefit to users by allowing selection of known minimotifs and predicted minimotifs for many human and rat Grb2 PPIs.

If two proteins are known to interact in human and rat, as in the case for Grb2, then it is reasonable to assume that they also interact in mouse and perhaps also in fly. When

Table IV

Comparison Between Filters Based on ROC Curves

	PPI filter	Frequency score filter
Area ^a	0.9	0.7
n.total ^b	22	16
n.events ^c	11	8
n.noevents ^d	11	8
<i>P</i> -value	0.001	0.08

^aArea is the area under the ROC curve.

^bn.total is the number of tests.

^cn.events is the total number of tests on true data.

^dn.noevents is the total number of tests on random (negative) data.

Table V

Percentages of Minimotifs in Grb2 that Pass Different PPI Filters

Grb2 ^a	PPI filter (%) ^b	HomoloGene-PPI filter (%) ^b
Human	36	36
Mouse	0	10
Rat	13	13
Fly	0	7

^aGrb2 proteins from different species were analyzed with the PPI and HomoloGene-PPI filters.

^bThe percentage of minimotif predictions that pass the filter.

we analyzed the same Grb2 proteins with the HomoloGene-filter, 10 and 7 minimotifs in mouse and fly Grb2, respectively, now passed the filter whereas none had passed the PPI filter (Table V). Although the HomoloGene-filter algorithm showed no distinct advantage when globally applied to MnM data, it is clear for the case of Grb2 that the filter worked as designed by extending minimotif predictions to proteins in other species.

We next examined the Similarity-PPI filter on the Grb2 proteins using different thresholds in BLAST to cluster proteins. Higher BLAST scores indicate more stringent protein similarity. Even when the highest BLAST threshold of 200 was used, we observed significantly more minimotifs passing the Similarity-PPI filter (Table VI). This result is consistent with more homologues being present in each protein cluster. As expected for all four species examined lower BLAST thresholds produced more predictions and the profiles were consistent with the variation in sensitivity, selectivity and score observed with when the BLAST threshold was titrated as shown in Figure 1.

Since the percentage of minimotifs was higher than expected for the Grb2 proteins, even at the highest BLAST threshold we implemented the additional constraint that S_i should contain p_i , the putative minimotif. Results from this algorithm shown in Table VII show that in all cases less minimotifs passed the filter than when there was no requirement for the presence of the minimotif in the Similarity PPI filter.

We wanted to develop a better feel for results we would obtain with a novel protein query. We randomly selected 100 proteins from the RefSeq database ((growth associated protein 43), CD2, DYRK1A, TRPM6, IRS-1,

Table VI

Percentages of Minimotifs in Grb2 that Pass the Similarity-PPI Filter

Grb2 ^a	BLAST score threshold ^b									
	10	20	30	40	50	100	150	200	500	1000
Human	74	63	61	59	55	55	55	55	55	55
Mouse	61	43	30	30	28	20	20	20	20	20
Rat	64	48	37	37	35	31	31	31	31	31
Fly	61	50	28	28	25	19	19	19	19	19

^aAnalysis as in Table V except that the Similarity PPI filter was used and BLAST threshold was varied to create different PPI datasets for the analysis.

Table VII

Percentages of Minimotifs in Grb2 that Pass the Similarity-PPI Filter that Contain the Predicted Minimotif

Grb2 ^a	BLAST score threshold ^a									
	10	20	30	40	50	100	150	200	500	1000
Human	55	44	42	36	36	36	36	36	36	36
Mouse	61	43	30	30	28	20	20	20	15	7
Rat	55	40	28	28	26	22	20	20	15	13
Fly	61	50	28	28	25	19	19	19	17	5

^aIn Analysis, as in Table VI except the additional constraint that S_i should contain p_b , the putative minimotif was implemented.

etc.) and analyzed them with Minimotif miner using the Similarity-PPI filters with different BLAST thresholds. When the homology filter was used with a promiscuous BLAST score threshold of 10, no predicted minimotifs were eliminated, whereas when stringent BLAST thresholds of 500 or 1000 were used, only 11% of the predictions were selected by the filter as having a previously known interaction in a related protein (Table VIII). Thus, a wide range of filtering was observed. The results are shown in the Appendix in a series of Tables.

We examine the putative minimotifs that were retained by the Similarity-PPI filter by examining IRS-1 target predictions. Several previously known interactions with IRS-1 were retained by the filter (Grb2, PI3K, insulin receptor, and epidermal growth factor receptor). In addition, a number of proteins with a related signaling function were also retained (Integrin, PTPN11, Fyn, Crk, Casein Kinase 2, and JAK2). These results indicate that the filter selects known positives and also identifies reasonable candidates for novel minimotif driven protein-protein interactions.

Adapting the Minimotif Miner 2 user interface to include PPI algorithms

To provide an interface for scientists to use the PPI filters, we added the PPI filter section to the Minimotif Miner 2.0 web application (Fig. 4). This filter section contains PPI, PPI-HomoloGene, and PPI-Similarity filters; BLAST thresholds of 10, 20, 30, 40, 50, 100, 150, 200, 500, and 1000 are available for the PPI-Similarity filter. For each filter, options to use the filter, examine and select motifs retained or eliminated by the filter are available. The PPI filters can be used in combinations with other minimotif scoring metrics. Furthermore, in addition to searching for minimotifs with previously known PPIs, the user can use the exclude option to also identify minimotifs that do not have a previously known PPI. Figures 5 and 6 show screen shots of the MnM website with and without the PPI filter; 48 of 75 minimotif predictions were eliminated by the filter in this analysis of acyl-CoA dehydrogenase.

The minimotif results table has also been modified to make each score column sortable by clicking at the top of

the column. This will better allow users to select the criteria they want to use to filter out false-positives or to focus their search. The MnM help section has been updated to help users with the new filter and reporting functions.

DISCUSSION

In developing a theory of PPIs, scientists have made significant progress in understanding the physical forces that drive chemical interactions and also have generated large datasets of known PPIs. Minimotifs can drive protein-protein interactions, thus provide a simplified system in which we begin to develop a protein-protein interaction theory.

Currently, there are no broad based tools with which a scientist can systematically search for protein-protein interactions that have minimotifs, an important tool for investigating the role of minimotifs in PPI theory. For example, if two proteins are known to interact, then identifying a minimotif in one that mediates an interaction with the other protein in the protein complex helps users formulate a hypothetical mechanism of the interaction. Since minimotif prediction has a high false-positive rate, this tool would have a second use in reducing false positives in the prediction of new minimotifs.

To address these problems, we have built several different PPI filters and implemented them in the Minimotif Miner 2 website.¹⁶ In building the PPI filters, we examined PPI data from existing PPI databases. When comparing the PPIs in the MnM database with known PPI databases that collectively have more than 500,000 interactions, we noticed that ~40% of the interactions in the MnM database were not yet observed in other PPI databases. Since the MnM annotation is a completely independent literature curation effort, this suggests, that even collectively the other existing PPI databases are not yet comprehensive for all PPIs reported in the literature.

In using the PPI filter, there was a strong preference for minimotifs being in protein with known PPI rather than randomly generated PPIs. In the example analysis of

Table VIII

Analysis of 100 Random Query Proteins with the Similarity-PPI Filter in MnM

Blast score threshold ^a	No. of not removed by filter ^a	Removed by filter (%) ^a
10	4658	28
20	2133	54
30	904	80
40	668	86
50	550	88
100	396	91
150	347	93
200	347	93
500	274	94
1000	274	94

^aAnalysis as in Table VI except on 100 randomly selected proteins.

MOTIF FILTERING	DOWNLOAD	
CHECK BOXES TO REQUIRE OR EXCLUDE MOTIFS		
Check 1st box to REQUIRE, or 2nd to EXCLUDE		
Motif Activities		
<input type="checkbox"/>	<input type="checkbox"/>	'Binds'
<input type="checkbox"/>	<input type="checkbox"/>	'Post-Translational'
<input type="checkbox"/>	<input type="checkbox"/>	'Requires'
Motif Sub-Activity		
<input type="checkbox"/>	<input type="checkbox"/>	'Trafficks'
<input type="checkbox"/>	<input type="checkbox"/>	'Phosphorylated'
<input type="checkbox"/>	<input type="checkbox"/>	'Proteolyzed'
Motif Class		
<input type="checkbox"/>	<input type="checkbox"/>	'Consensus'
<input type="checkbox"/>	<input type="checkbox"/>	'Instance'
Protein-Protein Interactions		
<input type="checkbox"/>	<input type="checkbox"/>	'PPIInteraction'
<input type="checkbox"/>	<input type="checkbox"/>	'PPI_homoloGene'
<input type="checkbox"/>	<input type="checkbox"/>	'PPI_Homology(10)'
<input type="checkbox"/>	<input type="checkbox"/>	'PPI_Homology(20)'
<input type="checkbox"/>	<input type="checkbox"/>	'PPI_Homology(30)'
<input type="checkbox"/>	<input type="checkbox"/>	'PPI_Homology(40)'
<input type="checkbox"/>	<input type="checkbox"/>	'PPI_Homology(50)'
<input type="checkbox"/>	<input type="checkbox"/>	'PPI_Homology(100)'
<input type="checkbox"/>	<input type="checkbox"/>	'PPI_Homology(150)'
<input type="checkbox"/>	<input type="checkbox"/>	'PPI_Homology(200)'
<input type="checkbox"/>	<input type="checkbox"/>	'PPI_Homology(500)'
<input type="checkbox"/>	<input type="checkbox"/>	'PPI_Homology(1000)'
Molecular/Cellular		
<input type="checkbox"/>	<input type="checkbox"/>	'Cellular 1'
<input type="checkbox"/>	<input type="checkbox"/>	'Cellular 2'
<input type="checkbox"/>	<input type="checkbox"/>	'Cellular 3'
<input type="checkbox"/>	<input type="checkbox"/>	'Molecular 1'
<input type="checkbox"/>	<input type="checkbox"/>	'Molecular 2'
<input type="checkbox"/>	<input type="checkbox"/>	'Molecular 3'
FILTER		

Figure 4

Image of filter selector and results modification added to the Minimotif Miner 2 web application. The category filters in the protein–protein interaction section was added for this article. [Color figure can be viewed in the online issue, which is available at wileyonlinelibrary.com.]

Grb2, 15 of the predictions with MnM that passed the PPI filter involved predictions that were not previously known to occur by the proposed mechanism. For example, several of the proteins that both interact with Grb2 and have a SH2 domain that binds to a consensus sequence that is consistent with a minimotif in Grb2 are Rasa (Y[ILV]x[FPYW]), Shp-1 (Y[IV]x[ILPV]) bLnk (Yxx[ILMP]), and Crk (YxxP). These proteins are predicted to bind at Tyr 209 near the end of the C-terminal SH3 domain of Grb2. Grb2 is also tyrosine phosphorylated on Tyr 209 (Human Protein Reference Database; HPRD), a requirement for these SH2 interactions.^{34,35} Examination of the structure of Grb2 (1GRI) shows that these minimotifs are on the surface and available for binding. Considering these data we can generate several new hypotheses for the mechanisms by which these proteins interact with Grb2, which is not yet known.

PPIs are very often conserved between similar species and are often conserved over a wider taxonomical range.³⁶ This is especially true in mammals where orthologous proteins in different species (which often have >90% amino acid identity) are inferred to have conserved interaction partners and minimotifs. The PPI-HomoloGene filter was designed to take advantage of PPI conservation, but did not show any improvement in discrimination ratio on the MnM data set when compared to the PPI filter; in fact it dropped significantly. We propose that this is due to that fact that most data in the MnM database does not have that same minimotif annotated for different species. This was supported by our analysis. The obvious need for this filter was evident in the analysis of Grb2. In Grb2, if one was studying a human protein 50% of the predictions pass this filter. This reflects that most work on Grb2 in the PPI databases was done in human and rat proteins. However, there were no proteins

Motifs Found

[X]	MOTIF EXPRESSION	ANNOTATION	OCCURRING POSITIONS	FREQ. SCORE	SURFACE P SCORE	# IN PROTEOME
	YASI	This consensus motif in IRS1 is dephosphorylated by SHP2; Tyr is dephosphorylated; fr	353	370.3	0.2	83
	YWIEVD	This consensus motif in peptide and pro-Interleukin 1 beta is proteolyzed by Caspase 1	342	331.4	0.7	154
	KxKx>	This consensus motif binds Coatamer and is trafficked to Endoplasmic Reticulum	418	205.9	0.0	289
	[TVIY]x[ASTV][QITVS][L]	This consensus motif in peptide binds the #2 SH2 domain of SHP-2; Tyr must be phosph	351	35.5	0.3	1492
	IYE	This instance motif in peptide is phosphorylated by eFPS; phosphorylated on Tyr; no m	399	31.7	0.7	1466
	TEY	This instance motif in Erk1 is phosphorylated by Mek; Thr and Tyr are phosphorylated; i	383	25.1	0.8	1300
	TxYxx[VI]	This consensus motif in CD2 binds the SH2 domain of SHP-1; Tyr must be phosphorylat	351	17.4	0.3	2475
	Y[FILM][FLMY][FLM]	This consensus motif binds the #2 FHA domain of Rad53; Tyr must be phosphorylated	201	17.3	0.0	3355
	[LV]x(1,5)Yx(1,5)[RK]	This consensus motif binds cholesterol; no modification required	63, 296, 332	16.0	0.7	97872
	YFx[FPLY]	This consensus motif in peptide binds the #1 SH2 domain of SHP-1; Tyr must be phosph	201	11.8	0.0	4389
	IAG	This instance motif in peptide is proteolyzed by MMP12, cleaves after Gly; no modificati	135	11.8	0.3	2504
	Y[AEV][YFESNV][PF][H]	This consensus motif in Lymphocyte cytosolic protein 2 binds the #1 SH2 domain of Ikk	353	9.2	0.2	4301
	IP[IV]	This consensus motif in alpha-Crystallin binds Alpha-Crystallin; no modification require	61	8.5	0.3	4811
	FxxLL	This consensus motif in peptide binds Androgen receptor; no modification required	309	6.9	0.4	7546
	G[KR][KR]	This consensus motif in PCMC is proteolyzed by Carboxypeptidase E; Removes C-term	234, 347	5.3	1.0	18843
	WE	This instance motif in OA1 binds unknown and is trafficked to Lysosomes	82, 342	5.3	1.0	14822
	MxxE	This consensus motif in Art1 binds Membrin and is trafficked to Golgi	149, 322, 328	4.8	0.8	24615
	Px[AP]xxR	This consensus motif binds the #1 SH3 domain of CIN85; no modification required	74	4.5	0.4	13129
	IY	This instance motif in peptide is phosphorylated by cFGR; phosphorylated on Tyr; no m	396, 399	4.4	0.5	23943
	CxxC	This consensus motif in Tim binds zinc and is trafficked to mitochondrial inner membran	156	4.2	0.0	27015
	TxxI	This consensus motif binds the FHA domain of Chk2; Thr must be phosphorylated	220, 228, 247, 403	4.2	0.8	39492
	[E/D]Y[ILV]	This consensus motif in peptide is phosphorylated by EGFR; Y residues is phosphorylat	182	4.1	0.3	11414
	[E/D]Y[ILV]	This consensus motif in peptide is phosphorylated by EGFR; phosphorylated on Tyr; no	182	4.0	0.3	11414
	DxxG	This consensus motif binds the G-protein domain of Phosphate; no modification require	68, 168, 227, 246, 2	3.8	1.0	49811
	[L]VExD	This instance motif is proteolyzed by Granzyme B; Cleaves after Asp; no modification re	224	3.7	0.5	10065
	[E]DYIY	This consensus motif in peptide is dephosphorylated by TC-PTP; Tyr is dephosphorylat	66, 72, 182, 352, 38	3.3	1.0	60894
	[L]V[L]MF[ILV]MF[IDE]	This consensus motif in AP2 beta binds Clathrin and is trafficked by internalization	312	3.2	0.3	11142
	YxN	This consensus motif in peptide binds the #1 SH2 domain of Grb2; Tyr must be phosphi	419	2.8	0.0	18279
	R[KR]x[ST]	This consensus motif in pyruvate kinase is phosphorylated by PKA; phosphorylation Ser	348	2.6	1.0	18387
	[AG][KR]	This consensus motif in Hepatocyte growth factor, Urokinase is proteolyzed by Matripas	6, 52, 58, 147, 196, :	1.9	1.0	267480
	ExT	This consensus motif in p27(Kip1) binds Skp2; Thr must be phosphorylated	40, 298, 401	1.9	1.0	57290
	YxL	This consensus motif binds the #2 FHA domain of Rad53; Tyr must be phosphorylated	201, 302	1.8	0.4	39809
	FxF	This consensus motif in WIP1 binds the #1 EVH1(WH1) domain of N-WASP; no modifia	37	1.8	0.6	24129
	HxxK	This consensus motif binds the #2 SH3 domain of GADS; no modification required	415	1.5	0.0	23574
	Rx[ST]	This consensus motif in pyruvate kinase is phosphorylated by PKA; phosphorylation Ser	148, 243, 306, 334, :	1.4	1.0	124575
	YxxP	This consensus motif in Crk binds the #1 SH2 domain of Crk; Tyr must be phosphorylat	73	1.4	0.6	24805
	[RK][RK]x[ST]	This consensus motif in 6-phosphofructo-2kinase is phosphorylated by PKG; phosphory	348	1.3	1.0	33840
	Yxx[IL]	This consensus motif binds the #2 SH2 domain of Syk; Tyr must be phosphorylated	201, 353	1.3	0.2	64849
	Y[LI]	This consensus motif in peptide binds the #1 SH2 domain of PLCgamma1; Tyr must be	145, 183	1.3	0.0	67601
	Txx[IL]	This consensus motif binds the #2 FHA domain of Rad53; Thr must be phosphorylated	220, 228, 247, 403	1.2	0.8	122582
	Yxx[ILMP]	This consensus motif in peptide binds the #1 SH2 domain of Blnk; Tyr must be phospho	73, 201, 353	1.2	0.6	98960
	Y[A/G/S/T/D/E]	This consensus motif is phosphorylated by Src; Y residues is phosphorylated; no modif	67, 114, 302, 353, 4	1.2	1.0	159389
	Y[TLV]FIC	This consensus motif in Growth hormone receptor binds the SH2 domain of Stat5; Tyr n	145, 158, 183, 201	1.2	0.0	150382
	SO	This instance motif in p53 (isoform a) is phosphorylated by ATM; phosphorylation Thr; r	22, 404	1.1	1.0	67558
	Yxx[FYL]	This consensus motif in transferrin receptor and LAMP1 binds AP1, AP2, AP3, AP4 mu st	201, 397	1.1	0.8	17138
	Yxx[ILM]	This consensus motif in T-cell receptor zeta chain binds the SH2 domain of Shc; Tyr mu	201, 353	1.1	0.2	74601
	MxxxL	This consensus motif in PSMA binds AP2 mu2 subunit, clathrin terminal domain, PTB dc	328	1.1	0.6	37376
	DxD	This consensus motif in glucuronyl transferase binds UDP/manganese; no modificatio	208	1.1	1.0	44122
	[PSAT]x[OEIE]	This consensus motif in CD40 binds the TRAF domain of TRAF2; no modification requir	56	1.0	0.8	47801
	[RK]xL	This consensus motif in Cyclin A binds Cdk2; no modification required	10, 144, 238, 294, 3	1.0	0.7	206191
	[TS]xxxx[VI]	This consensus motif in SLAM binds the SH2 domain of SH2D1A; no modification requir	70, 167, 228, 245, 3	1.0	0.7	221955
	[RK]x[RK]x(0,19)>	This consensus motif in glycosyl transferases binds Sar1 and is trafficked by Endoplasm	418	1.0	0.0	9136
	Yxx[VILFWYM]	This consensus motif in ITAM peptide motif binds the SH2 domain of ZAP70; Tyr must b	201, 353, 397	0.9	0.8	133580
	FxE	This consensus motif in MutS binds DNA; no modification required	41	0.9	0.7	40038
	YxxL	This consensus motif in CD46 binds AP complex and is trafficked by internalization	201	0.9	0.0	42342
	Yxx[LV]	This consensus motif in Jak2 is phosphorylated by JAK2; phosphorylated on Tyr; no m	201, 353	0.9	0.2	91611
	[HRK][ALSTV]x[ST]xx[DEF]	This consensus motif binds the #1 14-3-3 domain of 14-3-3epsilon; Ser must be phosph	217	0.8	0.4	50711
	[FILVW]xxxxxx[FILV]xxxx	This consensus motif binds the #1 Calmodulin domain of Calmodulin; no modification re	5, 48, 250, 270, 368	0.8	0.6	201280
	Txx[SA]	This consensus motif in peptide binds the FHA domain of KAPP; Thr must be phosphory	102, 300, 351	0.8	0.6	142153
	DG	This instance motif in vWF binds GPIb; no modification required	266	0.7	0.6	55499
	RxxK	This consensus motif binds the SH3 domain of GADS; no modification required	392	0.7	0.8	53665
	[KR]R	This consensus motif in mating factor is proteolyzed by Kexin2, cleaves after C-terminal	79, 348	0.7	1.0	128803
	RxxR	This consensus motif in proendothelin is proteolyzed by Prohormone Convertase 7; clea	7	0.6	0.3	70579
	TP	This instance motif in ELK-1 is phosphorylated by Erk; phosphorylation Ser/Thr; no mod	228	0.6	1.0	65125
	PxxxR	This consensus motif binds the #2 SH3 domain of Grb2; no modification required	76	0.6	0.6	68274
	Rxx[ST]	This consensus motif is phosphorylated by CamKII; phosphorylation Ser/Thr; no modif	13, 348	0.5	1.0	133630
	PxxP	This consensus motif in peptide binds the SH3 domain of SH3; no modification required	211	0.5	1.0	103587
	TxxxS	This consensus motif in Cyclin binds Skp1; Ser and Thr residues must be phosphorylate	351	0.5	0.4	78013
	[ST]xxE	This consensus motif is phosphorylated by Casein Kinase II; phosphorylation Ser; no m	121, 174	0.5	0.8	154187
	[KR]xx[ST]	This consensus motif in Psk is phosphorylated by RSK; phosphorylation Ser/Thr; no mo	13, 217, 348	0.4	1.0	251546
	[ST]xx[DE]	This consensus motif is phosphorylated by Casein Kinase II; phosphorylation Ser/Thr; n	121, 174, 207	0.4	0.8	256602
	[ST]xxx[ST]	This consensus motif in Glycogen synthase is phosphorylated by GSK3 beta; phospho	38, 117, 351	0.3	0.8	294800
	[ST]x[KR]	This consensus motif in peptide is phosphorylated by PKCalpha; phosphorylation Ser/Tl	51, 346	0.3	1.0	241478
	[ST]xxxS	This consensus motif in glycogen synthase is phosphorylated by GSK3 alpha; phospho	351	0.2	0.4	195351
	Sxx[ST]	This consensus motif is phosphorylated by Casein Kinase I; phosphorylation Ser/Thr; fir	22	0.2	0.8	201076

Figure 5

Screenshots of Results table in MnM. Image of results table from an MnM analysis of acyl-CoA dehydrogenase (NP_000007). MnM returns 75 minimotifs predictions. [Color figure can be viewed in the online issue, which is available at wileyonlinelibrary.com.]

Motifs Found						
[X]	MOTIF EXPRESSION	ANNOTATION	OCCURRING POSITIONS	FREQ. SCORE	SURFACE P SCORE	# IN PROTEOME
	YASI	This consensus motif in IRS1 is dephosphorylated by SHP2; Tyr is dephosphorylated; first	353	370.3	0.2	83
	[YW]EVD	This consensus motif in peptide and pro-Interleukin 1 beta is proteolyzed by Caspase 1 ; C	342	331.4	0.7	154
	KxKx>	This consensus motif binds Coatamer and is trafficked to Endoplasmic Reticulum	418	205.9	0.0	269
	[TV]YIYxY[ASTV]Q[ITVS]L	This consensus motif in peptide binds the #2 SH2 domain of SHP-2; Tyr must be phosphor	351	35.5	0.3	1492
	TxYxx[IV]	This consensus motif in CD2 binds the SH2 domain of SHP-1; Tyr must be phosphorylated	351	17.4	0.3	2475
	Y[FILM][FLMY][FLM]	This consensus motif binds the #2 FHA domain of Rad53; Tyr must be phosphorylated	201	17.3	0.0	3355
	YFx[FPLY]	This consensus motif in peptide binds the #1 SH2 domain of SHP-1; Tyr must be phosphor	201	11.8	0.0	4389
	[EDIY][LV]	This consensus motif in peptide is phosphorylated by EGFR; phosphorylated on Tyr; no m	182	4.0	0.3	11414
	[ILV]ExD	This instance motif is proteolyzed by Granzyme B; Cleaves after Asp; no modification requ	224	3.7	0.5	10065
	YxN	This consensus motif in peptide binds the #1 SH2 domain of Grb2; Tyr must be phosphoryl	419	2.6	0.0	18279
	ExT	This consensus motif in p27(Kip1) binds Skp2; Thr must be phosphorylated	40, 298, 401	1.9	1.0	57290
	YxL	This consensus motif binds the #2 FHA domain of Rad53; Tyr must be phosphorylated	201, 302	1.8	0.4	39809
	FxF	This consensus motif in WIP1 binds the #1 EVH1(WH1) domain of N-WASP; no modificati	37	1.8	0.6	24129
	HxxK	This consensus motif binds the #2 SH3 domain of GADS; no modification required	415	1.5	0.0	23574
	Txx[LL]	This consensus motif binds the #2 FHA domain of Rad53; Thr must be phosphorylated	220, 228, 247, 403	1.2	0.8	122582
	SQ	This instance motif in p53 (Isoform a) is phosphorylated by ATM; phosphorylation Thr; no r	22, 404	1.1	1.0	67558
	MxxxL	This consensus motif in PSMA binds AP2 mu2 subunit, clathrin terminal domain, PTB dom	328	1.1	0.6	37376
	[PSAT]x[QEIE]	This consensus motif in CD40 binds the TRAF domain of TRAF2; no modification required	56	1.0	0.8	47801
	[RK]xL	This consensus motif in Cyclin A binds Cdk2; no modification required	10, 144, 236, 294, 31	1.0	0.7	206191
	[RK]x[RK]x(0,19)>	This consensus motif in glycosyl transferases binds Sar1 and is trafficked by Endoplasmic	418	1.0	0.0	9136
	DG	This instance motif in vWf binds GPIb; no modification required	266	0.7	0.6	55499
	PxxxR	This consensus motif binds the #2 SH3 domain of Grb2; no modification required	76	0.6	0.6	66274
	TxxxS	This consensus motif in Cyclin binds Skp1; Ser and Thr residues must be phosphorylated	351	0.5	0.4	78013
	[ST]xxE	This consensus motif is phosphorylated by Casein Kinase II; phosphorylation Ser; no modi	121, 174	0.5	0.8	154187
	[ST]xx[DE]	This consensus motif is phosphorylated by Casein Kinase II; phosphorylation Ser/Thr; no n	121, 174, 207	0.4	0.8	256602
	[ST]x[KR]	This consensus motif in peptide is phosphorylated by PKCalpha; phosphorylation Ser/Thr;	51, 346	0.3	1.0	241476
	Sxx[ST]	This consensus motif is phosphorylated by Casein Kinase I; phosphorylation Ser/Thr; first :	22	0.2	0.8	201076

Figure 6

Screenshots of MnM website with PPI filter applied. Image of results table from an MnM analysis of specific acyl-CoA dehydrogenase (NP_000007) after applying the PPI filter. MnM returns 27 minimotif predictions after applying the PPI filter. [Color figure can be viewed in the online issue, which is available at wileyonlinelibrary.com.]

that passed this filter in mouse and fly orthologues. Since the domains and minimotifs are well conserved, we expect that any interaction observed in human and rat would likely also be observed in mouse, and likely fly orthologues. Thus, despite the poorer global performance of the PPI HomoloGene filter, it is clear that at least in isolated cases, it will be valuable to those studying PPIs and minimotifs.

Our initial implementation of the Similarity PPI filter showed that more minimotifs passed the filter than expected, even when high BLAST thresholds were used. This was not observed in the global analysis of the MnM data. Therefore, to adjust the stringency of this filter we provide users the option to use a wide range of BLAST thresholds, so that the number of resulting minimotifs can be adjusted on a case by case basis if desired. The related ROC curve and the *P*-value indicate that our algorithm is highly statistically significant. A comparison of the Similarity PPI filter with the previously reported frequency score filter indicates that the Similarity PPI filter is more significant statistically.¹⁵

In summary, the PPI, PPI-HomoloGene, and PPI-Similarity filters provide new computational tools to study the mechanisms of PPIs and to reduce false-positive prediction in the discovery of novel minimotifs.

For further details please see <http://mnm.engr.uconn.edu/>.

ACKNOWLEDGMENTS

We thank members of the Minimotif Miner team for critical input in the daily operations of our group.

REFERENCES

- Cornell WD, Cieplak P, Bayly CI, Gould IR, Merz KM Jr, Ferguson DM, Spellmeyer DC, Fox T, Caldwell JW, Kollman PA. A second generation force field for the simulation of proteins, nucleic acids, and organic molecules *J Am Chem Soc* 1995;117:5179–5197.
- Kennedy MA, McAteer K. Force field dependence of NMR-based, restrained molecular dynamics DNA structure calculations including an analysis of the influence of residual dipolar coupling restraints. *Abstr Pap Am Chem Soc* 2002;224:U482–U483.
- Case DA, Darden TA, Cheatham TE, III, Simmerling CL, Wang J, Duke RE, Luo R, Crowley M, Walker RC, Zhang W, Merz KM, Wang B, Hayik S, Roitberg A, Seabra G, Kolossvary I, Wong KF, Paesani F, Vanicek J, Wu X, Brozell SR, Steinbrecher T, Gohlke H, Yang L, Tan C, Mongan J, Hornak V, Cui G, Mathews DH, Seetin MG, Sagui C, Babin V, Kollman PA. AMBER 10. San Francisco: University of California; 2008.
- Lehne B, Schlitt T. Protein-protein interaction databases: keeping up with growing interactomes. *Hum Genomics* 2009;3:291–297.
- Mathivanan S, Periaswamy B, Gandhi TK, Kandasamy K, Suresh S, Mohmood R, Ramachandra YL, Pandey A. An evaluation of human protein-protein interaction data in the public domain. *BMC Bioinformatics* 2006;7Suppl 5:S19.
- Costanzo MC, et al. The Yeast Proteome Database (YPD) and Caenorhabditis elegans Proteome Database (WormPD): comprehensive resources for the organization and comparison of model organism protein information. *Nucleic Acids Res* 2000;28:73–76.
- Rivas JDL, Luis AD. Interactome data and databases: different types of protein interaction. *Comp Funct Genomics* 2004;5:173–178.
- Prieto C, Rivas JDL. APID: Agile Protein Interaction DataAnalyzer. *Nucleic Acids Res* 2006;34:W298–W302.
- Obenauer JC, Cantley LC, Yaffe MB. Scansite 2.0: proteome-wide prediction of cell signaling interactions using short sequence motifs. *Nucleic Acids Res* 2003;31:3635–3641.

10. Bailey TL, Williams N, Misleh C, Li WW. MEME: discovering and analyzing DNA and protein sequence motifs. *Nucleic Acids Res* 2006;34:W369–W373.
11. Lawrence CE, Altschul SF, Boguski MS, Liu JS, Neuwald AF, Wootton JC. Detecting subtle sequence signals: a Gibbs sampling strategy for multiple alignment. *Science* 1993;262:208–214.
12. Jonassen I. Efficient discovery of conserved patterns using a pattern graph. *Comput Appl Biosci* 1997;13:509–522.
13. Rigoutsos I, Floratos A. Combinatorial pattern discovery in biological sequences: the TEIRESIAS algorithm. *Bioinformatics* 1998;14: 55–67.
14. Tan SH, Willy H, Sung WK, Ng SK. A correlated motif approach for finding short linear motifs from protein interaction networks. *BMC Bioinformatics* 2006;7:502.
15. Balla S, Thapar V, Luong T, Faghri T, Huang CH, Rajasekaran S, del Campo JJ, Shin JH, Mohler WA, Maciejewski MW, et al. Minimotif Miner, a tool for investigating protein function. *Nat Methods* 2006;3:175–177.
16. Rajasekaran S, Balla S, Gradie P, Gryk MR, Kadaveru K, Kundeti V, Maciejewski MW, Mi T, Rubino N, Vyas J, Schiller MR. Minimotif miner 2nd release: a database and web system for motif search. *Nucleic Acids Res* 2009;37 (Suppl 1):D185–D190.
17. Gould CM, Diella F, Via A, Puntervoll P, Gemünd C, Chabanis-Davidson S, Michael S, Sayadi A, Bryne JC, Chica C, et al. ELM: the status of the 2010 eukaryotic linear motif resource. *Nucleic Acids Res* 2010;38:D167–D180.
18. Via A, Gould CM, Gemünd C, Gibson TJ, Helmer-Citterich M. A structure filter for the Eukaryotic Linear Motif Resource. *BMC Bioinformatics* 2009;10:351.
19. Neduva V, Russell RB. Linear motifs: evolutionary interaction switches. *FEBS Lett* 2005;579:3342–3345.
20. Songyang Z, Shoelson SE, Chaudhuri M, Gish G, Pawson T, Haser WG, King F, Roberts T, Ratnofsky S, Lechleider RJ, et al. SH2 domains recognize specific phosphopeptide sequences. *Cell* 1993;72: 767–778.
21. Wu C, Ma MH, Brown KR, Geisler M, Li L, Tzeng E, Jia CY, Jurisica I, Li SS. Systematic identification of SH3 domain-mediated human protein-protein interactions by peptide array target screening. *Proteomics* 2007;7:1775–1785.
22. Aranda B, Achuthan P, Alam-Faruque Y, Armean I, Bridge A, Derow C, Feuermann M, Ghanbarian AT, Kerrien S, Khadake J, Kersemakers J, Leroy C, Menden M, Michaut M, Montecchi-Palazzi L, Neuhauser SN, Orchard S, Perreau V, Roehert B, van Eijk K, Hermjakob H. The IntAct molecular interaction database in 2010. *Nucleic Acids Res* 2010;38:D525–D531.
23. Chatr-aryamontri A, Ceol A, Peluso D, Nardozza A, Panni S, Sacco F, Tinti M, Smolyar A, Castagnoli L, Vidal M, et al. VirusMINT: a viral protein interaction database. *Nucleic Acids Res* 2009;37:D669–D673.
24. Vyas J, Nowling RJ, Maciejewski MW, Rajasekaran S, Gryk MR, Schiller MR. A proposed syntax for minimotif semantics, version 1. *BMC Genomics* 2009;10:360.
25. Ren S, Uversky VN, Chen Z, Dunker AK, Obradovic Z. Short Linear Motifs recognized by SH2, SH3 and Ser/ThrKinase domains are conserved in disordered protein regions. *BMC Genomics* 2008;9 (Suppl 2):S26.
26. Chica C, Diella F, Gibson TJ. Evidence for the concerted evolution between short linear protein motifs and their flanking regions. *PLoS One* 2009;4:e6052.
27. Edwards RJ, Davey NE, Shields DC. SLiMfinder: a probabilistic method for identifying over-represented, convergently evolved, short linear motifs in proteins. *PLoS One* 2007;2:e967.
28. Sayers EW, et al. Database resources of the National Center for Biotechnology Information. *Nucleic Acids Res* 2009;37:D5–D15.
29. Altschul SF, Gish W, Miller W, Myers EW, Lipman DJ. A basic local alignment search tool. *J Mol Biol* 1990;215:403–410.
30. R Development Core Team. R: a language and environment for statistical computing. *R Foundation Stat Comput* 2009;1:1650.
31. Mason SJ, Graham NE. Areas beneath the relative operating characteristics (ROC) and relative operating levels (ROL) curves: statistical significance and interpretation. *QJR Meteorol Soc* 2002;30:291–303.
32. Bamber D. The area above the ordinal dominance graph and the area below the receiver-operating characteristic graph. *J Math Psychol* 1975;12:387–415.
33. Hanley JA. The robustness of the ‘binormal’ assumptions used in fitting ROC curves. *Med Decision Making* 1988;8:197–203.
34. Li L, Wu C, Huang H, Zhang K, Gan J, Li SS. Prediction of phosphotyrosine signaling networks using a scoring matrix-assisted ligand identification approach. *Nucleic Acids Res* 2008;10:3263–3273.
35. Machida K, et al. High-throughput phosphotyrosine profiling using SH2 domains. *Mol Cell* 2007;26:899–915.
36. Choi YS, Yang JS, Choi Y, Ryu SH, Kim S. Evolutionary conservation in multiple faces of protein interaction. *Proteins: Struct Funct Bioinform* 2009;77:14–25.
37. Salwinski L, Miller CS, Smith AJ, Pettit FK, Bowie JU, Eisenberg D. The database of interacting proteins: 2004 update. *Nucleic Acids Res* 2004;32:D449–D451.
38. Maglott D, Ostell J, Pruitt KD, Tatusova T. Entrez Gene: gene-centered information at NCBI. *Nucleic Acids Res* 2007;35:D26–D31.
39. Keshava Prasad TS, Goel R, Kandasamy K, Keerthikumar S, Kumar S, Mathivanan S, Telikicherla D, Raju R, Shafreen B, Venugopal A, Balakrishnan L, Marimuthu A, Banerjee S, Somanathan DS, Sebastian A, Rani S, Ray S, Harrys Kishore CJ, Kanth S, Ahmed M, Kashyap MK, Mohmood R, Ramachandra YL, Krishna V, Rahiman BA, Mohan S, Rangannathan P, Ramabadran S, Chaerkady R, Pandey A. Human Protein Reference Database—2009 update. *Nucleic Acids Res* 2009;37:D767–D772.
40. Ceol A, Chatr Aryamontri A, Licata L, Peluso D, Briganti L, Perfetto L, Castagnoli L, Cesareni G. MINT, the molecular interaction database: 2009 update. *Nucleic Acids Res* 2010;38:D532–D539.

APPENDIX

Pseudocode for HomoloGene-PPI filter

Input: Query Protein Q , a Set of Target Proteins T_1, \dots, T_n .

Algorithm:

- Get the homologue cluster for Q . Let it be $\{Q_1, Q_2, \dots, Q_n\}$.
- For each $i = 1$ to n do

Get the interactors of Q_i from the database. This results in the set $\{Q_{p1i}, Q_{p2i}, \dots, Q_{pim}\}$. Now we have the interactor pairs as set Q' as follows:

$$\{(Q_1, Q_{p11}), (Q_1, Q_{p12}), \dots, (Q_1, Q_{p1m})\}$$

$$\{(Q_2, Q_{p21}), (Q_2, Q_{p22}), \dots, (Q_2, Q_{p2m}),$$

$$\dots,$$

$$\{(Q_n, Q_{pn1}), (Q_n, Q_{pn2}), \dots, (Q_n, Q_{pnm})\}$$

- Remove from Q' all pairs that are not of the same species, to get Q'' .
- For each $i = 1$ to n do

Get the homologue cluster of target protein T_i . Let it be $\{T_{i1}, T_{i2}, \dots, T_{im}\}$.

For each $j = 1$ to m do

Check if there exists a pair in Q'' such that $Q_{pxy} = T_{ij}$.

If yes, (Q, T_i) passes the filter. Else it fails.

Pseudocode for Similarity-PPI filter

Input: Query Protein Q , a set of Target Proteins (T_1, \dots, T_n) , Threshold t , PPI Databases with interactors as $\{(I_1, I_1'), (I_2, I_2') \dots \{I_x, I_x'\}\}$

Algorithm:

- Blast Q against all the entries in the database. Get all the entries within the threshold. Let the resulting set be $S\{s_1, s_2, s_3, \dots, s_n\}$. (S has, say example, $\{I_3, I_7', I_{15}, I_{19}, I_{34}', \dots\}$)
- For each $i = 1$ to n in S do

Get the interacting pair of interactors from the database. Say if the interactors is I_1 , then get I_1' . The resulting set of all the partners of interactors in S be S' . (Now S' has entries $\{I_3', I_7, I_{15}', I_{19}', I_{34}, \dots\}$)

- For each $i = 1$ to n do

Blast the target T_i against S' .

If the score is within the threshold t , (Q, T_i) passes the filter. Else it fails.